JCBI
Journal of Computing & Biomedical Informatics
ISSN: 2710 - 1606
Volume 06 Issue 02
2024

Research Article
https://doi.org/10.56979/602/2024

A Multimodal Approach for Alzheimer's Disease Detection and Classification Using Deep Learning

Ali Hassan[1], Azhar Imran[1*], Aman Ullah Yasin[1], Muhammad Ahmad Waqas[2], and Rabeeha Fazal[3]

[1]Department of Creative Technologies, Air University, Islamabad, 44000, Pakistan.
[2]Department of Information Technology, Govt Collage University Faisalabad, Pakistan.
[3]Department of Information Security, Comsats University Islamabad, 44000, Pakistan.
[*]Corresponding Author: Azhar Imran. Email: azhar.imran@au.edu.pk

Received: January 05, 2024 **Accepted:** February 28, 2024 **Published:** March 01, 2024

Abstract: Alzheimer's disease (AD) presents a substantial challenge to healthcare systems globally due to its progressive nature and the absence of effective treatments. The timely identification of AD is crucial for enabling interventions aimed at potentially slowing cognitive decline and enhancing patient outcomes. Recent advancements in medical imaging, notably PET and MRI, provide valuable insights into the subtle changes associated with AD pathology. This study investigates the utilization of the VGG16 deep learning model, recognized for its proficiency in image recognition tasks, to extract detailed features from MRI and PET scans. By leveraging the capabilities of deep learning, our objective is to reveal subtle patterns indicative of AD pathology. These extracted features are consolidated into a unified representation, which facilitates the training of machine learning classifiers. Employing various classifiers, such as Random Forest, Support Vector Machine, and K-Nearest Neighbors, we aim to exploit their strengths in managing complex data. The experimental outcomes demonstrate the effectiveness of this hybrid approach, with the Support Vector Machine emerging as the most successful classifier, achieving an accuracy of 84%. These findings underscore the potential of deep learning-assisted feature extraction and emphasize the significance of integrating advanced imaging techniques with sophisticated machine learning algorithms for improved AD detection and classification. Such initiatives hold promise for advancing our comprehension of AD pathology, enhancing diagnostic precision, and ultimately contributing to more effective management strategies for this debilitating neurological disorder.

Keywords: Early detection of Alzheimer's disease (AD); diagnostic imaging in healthcare; Integrative methodology; Integratigration of Deep Learning with Machine Learning in Alzheimer's disease; Integration of MRI and PET scans.

1. Introduction

PET imaging plays a crucial role in detecting changes in the brain associated with Alzheimer's disease (AD), particularly in metabolic processes and the accumulation of amyloid-beta (Aβ) plaques. The introduction of PET tracers like Pittsburgh compound B (PiB) has significantly aided in visualizing Aβ plaques, a key feature of AD pathology [1]. Moreover, the emergence of new PET tracers targeting tau protein accumulation provides deeper insights into neurofibrillary tangles, another critical aspect of AD pathology [2].

MRI offers a complementary perspective, utilizing its high spatial resolution to identify structural brain alterations indicative of AD. Research emphasizes the importance of structural MRI in detecting markers such as hippocampal volume and cortical thickness, serving as indicators of AD-related neurodegeneration [3]. Additionally, advanced MRI techniques such as diffusion tensor imaging (DTI)

offer insights into microstructural changes in white matter, enhancing our understanding of the underlying mechanisms of AD [4].

The integration of PET and MRI imaging holds significant promise in improving the accuracy of AD detection and classification. This multimodal approach provides a comprehensive view of AD pathology, combining evidence of amyloid and tau pathology with structural brain changes, facilitating the differentiation of AD from other neurodegenerative conditions [5].

Machine learning techniques have increasingly played a role in analyzing PET and MRI data, leading to more automated and objective diagnostic processes. For example, support vector machine (SVM) algorithms have successfully distinguished AD patients from healthy controls using PET imaging markers [6], while convolutional neural networks (CNNs) have automated the feature extraction and classification processes from MRI data, promising more efficient diagnostics [7].

However, challenges persist on the path to perfecting AD detection and classification through PET and MRI, including the necessity for standardized imaging protocols and biomarker quantification to ensure consistency across studies [8]. The pursuit of reliable imaging-based biomarkers capable of predicting clinical outcomes and monitoring disease progression remains crucial in combating Alzheimer's disease [9].This evolving landscape of AD diagnosis, fueled by technological advancements and interdisciplinary collaboration, is paving the way for more effective management and intervention strategies, potentially revolutionizing patient care and outcomes in the realm of neurodegenerative diseases.

In this paper, a hybrid Deep Learning Approach for the early detection of Alzheimer's disease (AD) is presented, combining multimodal imaging and Convolutional Neural Network (CNN) with Long Short-term Memory (LSTM) algorithm [5]. The methodology integrates magnetic resonance imaging (MRI), positron emission tomography (PET), and neuropsychological test scores, achieving a remarkable accuracy of 98.5% in distinguishing cognitively normal controls from early mild cognitive impairment (EMCI) [10]. This highlights the potential of deep neural networks to automatically identify AD indicative biomarkers. Additionally, a deep CNN model for AD diagnosis utilizing brain MRI data analysis is proposed [11].Unlike binary classification approaches, this model can identify various stages of AD and demonstrates superior performance, outperforming comparative baselines on the Open Access Series of Imaging Studies dataset [12]. Furthermore, the paper discusses recent advancements in deep learning technology, particularly in the analysis of functional MRI (fMRI) for AD diagnosis, highlighting the potential of deep learning methods to aid in AD diagnoses [13]. Transfer learning techniques using pre-trained weights from benchmark datasets coupled with image entropy selection are explored to enhance the efficiency of AD detection with smaller training sizes [14]. Moreover, the utilization of MRI coupled with K-Means Clustering and Watershed method for hippocampus segmentation shows promising results in AD detection, contributing to the growing body of research aiming to improve early diagnosis and treatment outcomes for AD patients [15]. The presented research explores various approaches to improve the diagnosis of Alzheimer's Disease (AD) through innovative methodologies integrating multimodal medical imaging data. Firstly, the CMPGAN model is introduced, aiming to address issues like mode collapse and gradient disappearance common in traditional generative models [16]. This model utilizes consistent manifold projection and a novel distribution distance metric to project data onto low-dimensional manifolds effectively. Additionally, a feature extraction network is developed, incorporating radial medley units for multiscale feature extraction and harmonic voxel fusion matrix for voxel-level feature extraction. Experimental results demonstrate the effectiveness of this approach in FDG-PET generation and AD diagnosis, offering potential guidance for clinicians.

Another aspect addressed in the paper is the challenge of non-intuitive data fusion in imaging genetics studies for AD. A multi-modal data fusion framework called MFASN is proposed, leveraging deep auto-encoder and self-representation techniques [17]. This framework constructs a multi-modality brain network from fMRI and sMRI data, utilizes deep auto-encoder for non-linear transformations and feature selection, incorporates sparse self-representation to capture multi-subspaces structure, and employs a multi-task structured sparse association model to mine correlations between genetic data and brain network features.

The proposed method outperforms existing approaches, aiding in the discovery of discriminative biomarkers associated with AD. Furthermore, the study investigates classification models using 2D and

3D MRI images alongside amyloid PET scans, both individually and in multi-modal frameworks. Results indicate that models incorporating volumetric data and integrating multiple modalities exhibit superior performance, with state-of-the-art results achieved on the OASIS-3 cohort [18]. Additionally, explainability analyses highlight the models' focus on crucial AD-related regions, enhancing understanding of the disease's mechanisms.

The paper also presents a comprehensive comparison of statistical machine learning methods for AD diagnosis, exploring different data fusion strategies and dimensionality reduction techniques[19]. A novel supervised encoder method is introduced, demonstrating substantial improvement in prediction accuracy, particularly in combination with intermediate fusion for multiclass diagnosis prediction.

Lastly, a novel Generative Adversarial Network incorporating a pyramidal attention mechanism is proposed to address the lack of PET image data in AD diagnosis datasets[20]. This approach generates PET images [21-24].

2. Materials and Methods

This section thoroughly describes the tools, techniques, and protocols employed for data collection, processing, and analysis, ensuring transparency and reproducibility in the research findings.

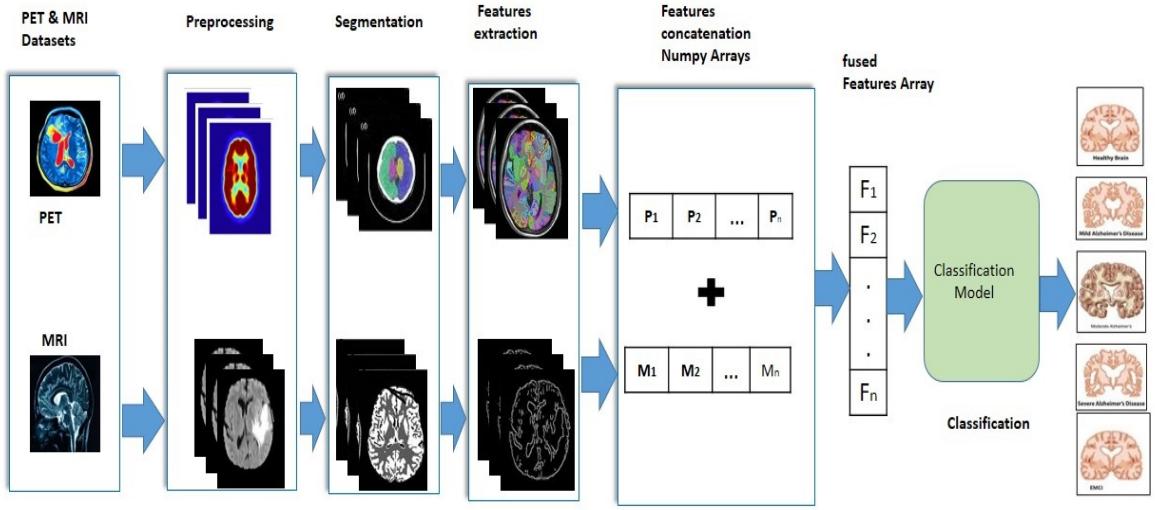

Figure 1. Proposed Methodology Block diagram

2.1. MRI & PET Datasets

The research utilized two distinct datasets containing MRI and PET images of the brain, sourced from the Alzheimer's Disease Neuroimaging Initiative (ADNI) database. These datasets consist of images categorized into five classes: Mild Cognitive Impairment (MCI), Cognitively Normal (CN), Early Mild Cognitive Impairment (EMCI), Late Mild Cognitive Impairment (LMCI), and Alzheimer's Disease (AD). The MRI dataset includes 400 images for MCI, 300 for CN, 200 for EMCI, 240 for LMCI, and 180 for AD. Meanwhile, the PET dataset comprises 300 images for MCI, 250 for CN, 190 for EMCI, 292 for LMCI, and 288 for AD. In total, there are 2640 images available for feature extraction across all classes. This diverse dataset facilitates comprehensive analysis and exploration of the pathological signatures associated with each class, supporting the development of robust diagnostic and classification models for Alzheimer's disease.

Table 1. PET & MRI Datasets

Datasets	MCI	CN	EMCI	LMCI	AD	Total
MRI	400	300	200	240	180	**1320**
PET	300	250	190	292	288	**1320**
MRI+PET			**2640**			

2.2. Preprocessing

The described image preprocessing method adopts a systematic approach to enhance image quality for further analysis [25-27]. Initially, it standardizes image dimensions to 256x256 pixels to ensure consistency across datasets. Following this, Gaussian smoothing is applied using a 5x5 kernel to reduce noise while preserving important features. This helps in mitigating the impact of random variations in the image. The final enhancement step involves adaptive histogram equalization, specifically employing a contrast-limited adaptive Histogram Equalization (CLAHE) algorithm. This algorithm is fine-tuned for both clip limit and tile grid size to improve the contrast of the images. Enhancing contrast is critical for highlighting subtle features and enhancing the visibility of important structures within the images [28-30]. By implementing these techniques in sequence, the method effectively prepares images for detailed examination and analysis, particularly in fields requiring precise diagnostic or analytical insights from visual data.

2.3. Segmentation

The application of a Fully Convolutional Network (FCN) for segmenting PET and MRI datasets involves a mathematical model comprising convolutional layers followed by up sampling layers. The objective is to produce precise pixel-wise predictions. Let XPET represent the input PET image dataset and XMRI represent the input MRI image dataset. The structure of the FCN can be described as follows:

$$YPET = fPET(XPET) \quad (1)$$

$$YMRI = fMRI(XMRI) \quad (2)$$

In this context, $\mathbf{f_{PET}}$ and $\mathbf{f_{MRI}}$ represent the functionalities of the FCN models customized for PET and MRI datasets, respectively. These functionalities incorporate convolutional layers for feature extraction and upsampling layers to support pixel-wise forecasting. The resulting $\mathbf{Y_{PET}}$ and $\mathbf{Y_{MRI}}$ outputs materialize as dense prediction maps, outlining segmented areas of interest within the PET and MRI images.

2.4. Features Extraction & Fusion

Feature extraction is a pivotal step in computer vision and medical imaging, focusing on discerning and isolating significant patterns or attributes within visual data. Its objective is to distill specific characteristics, such as pixel intensities or textures, to represent data in a more meaningful and manageable manner. This process aids in reducing data dimensionality while retaining pertinent information, thereby facilitating diverse analysis tasks like object recognition and classification [31-34]. The methodologies for feature extraction are manifold, tailored to the unique characteristics of image data and the requirements of specific applications. They assume a critical role in advancing the comprehension and analysis of visual data across various fields, notably in medical imaging, where they contribute to the identification and characterization of anomalies and diseases. Moreover, the integration of features from different sources or modalities, known as feature fusion, further enhances the representation of visual data, enabling a more comprehensive analysis and deeper insights.

2.4.1. VGG-16

To initiate the process, essential libraries are imported, including OpenCV for image processing and the Keras framework for deep learning functionalities. The load_images function is then utilized to navigate through the specified directory and load MRI and PET images, discerning between them based on filenames. Following this, the images undergo resizing to meet the input size requirements of the VGG16 model (224x224 pixels) and are converted into NumPy arrays for further processing. Subsequently, the script transforms the lists of features extracted from both MRI and PET images into NumPy arrays, facilitating efficient storage and manipulation. These arrays can then be used as inputs for subsequent analysis tasks, such as Alzheimer's disease classification or prediction. By employing deep learning models for feature extraction, researchers can harness the representational capabilities of convolutional neural networks (CNNs), enabling the automatic acquisition of discriminative features directly from raw image data. Additionally, adjusting parameters like batch size, step size, and the number of epochs can fine-tune the feature extraction process to enhance the model's performance. In our approach, we employed 30 epochs with a step size of 20 and a learning rate of 0.01, aiming to optimize the training process and facilitate model convergence while balancing computational efficiency.

For PET images:
Let $\boldsymbol{P_a}$ shows the number of PET images.
Let $\boldsymbol{Fp}$ represent the feature array extracted from each PET image.
The application of the VGG16 model to PET images can be symbolized as**:**

$$VGG16(P_a) = \{Fp1, Fp2, \ldots, FpP\} \quad (3)$$

For MRI images:
Let M_a denote the number of MRI images.
Let Fm represent the feature array extracted from each MRI image.
The VGG16 model applied to MRI images can be represented as:

$$VGG16(M_a) = \{Fm1, Fm2, \ldots, FmM\} \quad (4)$$

For feature fusion:
Let concat describe the concatenation operation.
The fusion of PET and MRI features using VGG16 can be expressed as:

$$VGG16fusion = concat(VGG16(P_a), VGG16(M_a)) \quad (5)$$

In this context, "VGG16fusion" denotes the amalgamated feature set comprising features extracted from PET and MRI images using the VGG16 model.

2.5. Classification

In the classification section, we explore the utilization of machine learning algorithms for the differentiation of various classes or categories of data. Our emphasis lies in employing diverse classifiers to identify patterns and relationships within the extracted features, enabling precise classification between Alzheimer's disease cases and healthy controls.

2.5.1. KNN

The K-Nearest Neighbors (KNN) algorithm is recognized for its simplicity and effectiveness in classification tasks. It assigns a sample to a particular category by examining the class labels of its k nearest neighbors. Unlike some other algorithms, KNN doesn't rely on a specific equation; instead, it calculates distances between data points to gauge their proximity. In the context of MRI and PET feature arrays, KNN computes the distance between the query point, which represents the combined MRI and PET features of a sample, and all other points in the feature space. The class label of the query point is then determined based on the majority class among its k nearest neighbors.

The equation for the K-Nearest Neighbors (KNN) algorithm when applied to MRI and PET feature arrays involves computing the distance between the query sample and all other samples in the feature space. Let X_{mri} and X_{PET} represent the MRI and PET feature arrays, respectively, each containing N samples with D_{MRI} and D_{PET} features, respectively. The distance metric used, typically Euclidean distance, is calculated as:

$$Distance(x_i, x_q) = \sqrt{\sum_{j=1}^{D_{MRI}} \left(x_{MRI,ij} - x_{MRI,qj}\right)^2_+ \sum_{K=1}^{D_{PET}} \left(x_{PET,ik} - x_{PET,qk}\right)^2} \quad (6)$$

2.5.2. SVM

Support Vector Machine (SVM) serves as a robust supervised learning method widely used for classification tasks. Its primary objective is to determine the optimal hyperplane capable of effectively separating data points into distinct classes based on their features. In the context of the linear kernel variant of SVM, it establishes a linear decision boundary to delineate classes.
The SVM equation is denoted as:

$$y = sign(W_{fused} \cdot X_{(MRI,PET)} + b_{fused}) \quad (7)$$

Where sign(W_{fused}) represents the weight vector, sign$\left(X_{(MRI,PET)}\right)$ denotes the feature vector, b_{fused} is the bias term, and y signifies the predicted class label. When applied to MRI and PET features, represented as numpy arrays, the equation remains consistent, with $X_{(MRI,PET)}$ representing the concatenated feature vector comprising both MRI and PET features.

2.5.3. Random Forest

When utilizing Random Forest for classification with two NumPy arrays of MRI and PET features, the algorithm employs these features as input to a collection of decision trees. Unlike linear models, Random Forest does not adhere to a single equation. Instead, it amalgamates the predictions from numerous decision trees within the ensemble. Consequently, the equation for Random Forest involves amalgamating the decision rules from each tree to determine the final classification outcome. Mathematically, this aggregation process can be represented as follows:

$$\hat{y} = mode(y1, y2, \ldots, yn) \quad (8)$$

Where In our study, e ^y denotes the predicted class, and $y1, y2, \ldots, yn$ represent the individual predictions from each decision tree in the Random Forest ensemble. The mode function selects the most frequently occurring class among these predictions to assign the final classification label. We utilized 100 estimators for the Random Forest classifier, indicating the number of decision trees generated within the ensemble. By employing a larger number of estimators, our aim was to improve the predictive performance of the model by aggregating predictions from a diverse set of decision trees, thereby enhancing the overall robustness and accuracy of the classification results.

3. Results

In the results section, we outline the outcomes obtained from utilizing three separate classification algorithms: K-nearest neighbors (KNN), Support Vector Machine (SVM), and Random Forest. Each algorithm's performance is assessed concerning the classification of MRI and PET features for Alzheimer's disease detection. This section emphasizes the achieved accuracies of each algorithm, offering insights into their efficacy in discerning between various disease states. Furthermore, the results illuminate the relative strengths and limitations of these classification methodologies, providing valuable implications for future research and clinical implementations in Alzheimer's disease diagnosis.

3.1. SVM

Among the classification models studied, the Support Vector Machine (SVM) emerged as the top performer, achieving an accuracy of 84%. The corresponding loss value, which reflects the model's predictive error, was recorded at 0.380. Analysis of the confusion matrix, which visually depicts the model's predictions compared to the actual labels, offers valuable insights into its classification performance across different disease states. The high accuracy achieved by SVM underscores its effectiveness in identifying patterns within the MRI and PET feature space associated with Alzheimer's disease. This strong performance emphasizes SVM's potential as a dependable tool for early detection and classification tasks in Alzheimer's research and clinical practice, presenting promising avenues for further investigation and application in disease management strategies.

Figure 2. SVM accuracy ,loss & confusion Matrix

3.2. KNN

In our experimentation, we utilized the K-Nearest Neighbors (KNN) algorithm, achieving an accuracy rate of 80% and a corresponding loss value of 2.08. KNN operates based on proximity, assigning a data point the most common class label among its nearest neighbors. The parameter 'k', representing the number of neighbors, significantly affects the model's effectiveness. For our study, we selected k to be 3, meaning the algorithm considers the labels of the three closest neighbors when making predictions. The confusion matrix visually illustrates the model's predicted labels versus the true labels, providing insights into its classification performance across various disease states.

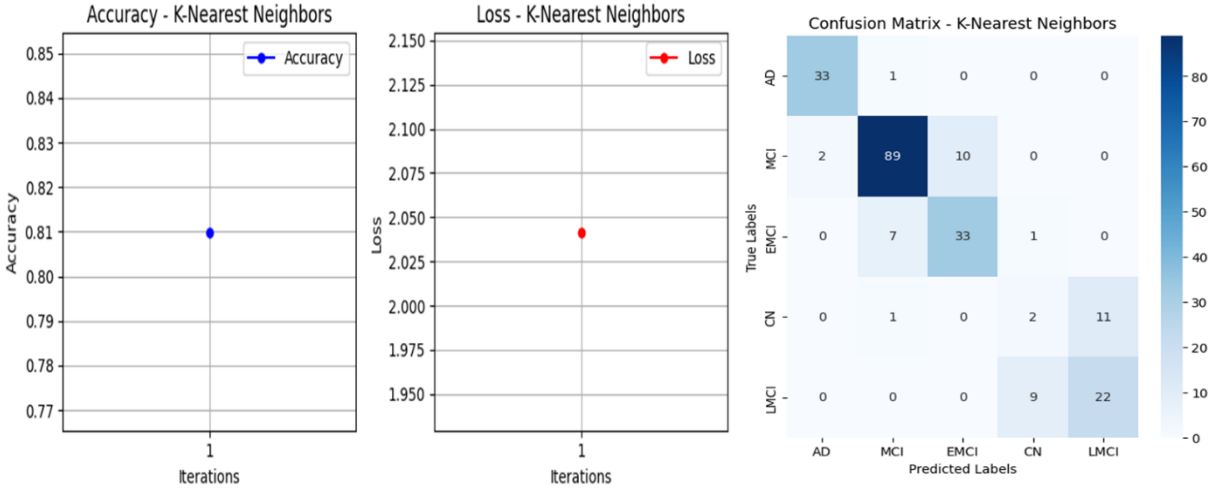

Figure 3. KNN accuracy ,loss & confusion Matrix

3.3. Random Forest

The Random Forest (RF) algorithm achieved a classification accuracy of 73% in distinguishing between different disease states in Alzheimer's detection. Furthermore, the corresponding loss value was recorded at 0.88, indicating the variance between predicted and actual labels. The confusion matrix visually illustrates the predicted labels against the ground truth labels, providing insights into the algorithm's performance across various classes. With the utilization of 100 estimators in the Random Forest model, our goal was to utilize ensemble learning to bolster the robustness and predictive capability of the classification process [35-38]. These observations highlight the effectiveness of Random Forest in addressing intricate classification tasks and its potential applicability in Alzheimer's disease diagnosis and research efforts.

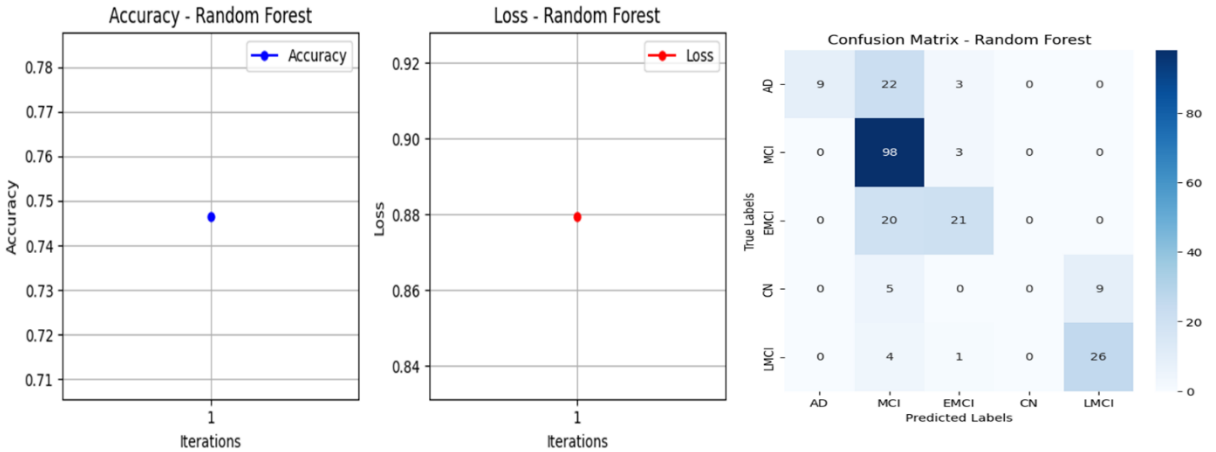

Figure 4. Random Forest accuracy ,loss & confusion Matrix

4. Discussion

In comparison with previous studies, our analysis identified significant variations in the performance of machine learning algorithms—specifically K-Nearest Neighbors (KNN), Support Vector Machine (SVM), and Random Forest (RF)—in the classification of Alzheimer's disease. KNN achieved a classification accuracy of 80%, surpassing both SVM and RF. SVM attained an accuracy of 84%, while RF

demonstrated a slightly lower accuracy rate of 73%. Despite SVM's superior accuracy, it incurred longer computation times due to its reliance on instance-based learning. Conversely, both KNN and RF offered quicker processing times, with RF particularly noteworthy for its ensemble learning approach and adeptness in handling complex classification tasks. Moreover, although KNN and RF encountered some misclassification errors, RF exhibited enhanced robustness in predictive capabilities. These findings shed light on the intricate balance between classification accuracy, computational efficiency, and model resilience inherent in various machine learning algorithms. Such insights are invaluable for advancing research in Alzheimer's disease detection and classification methodologies.

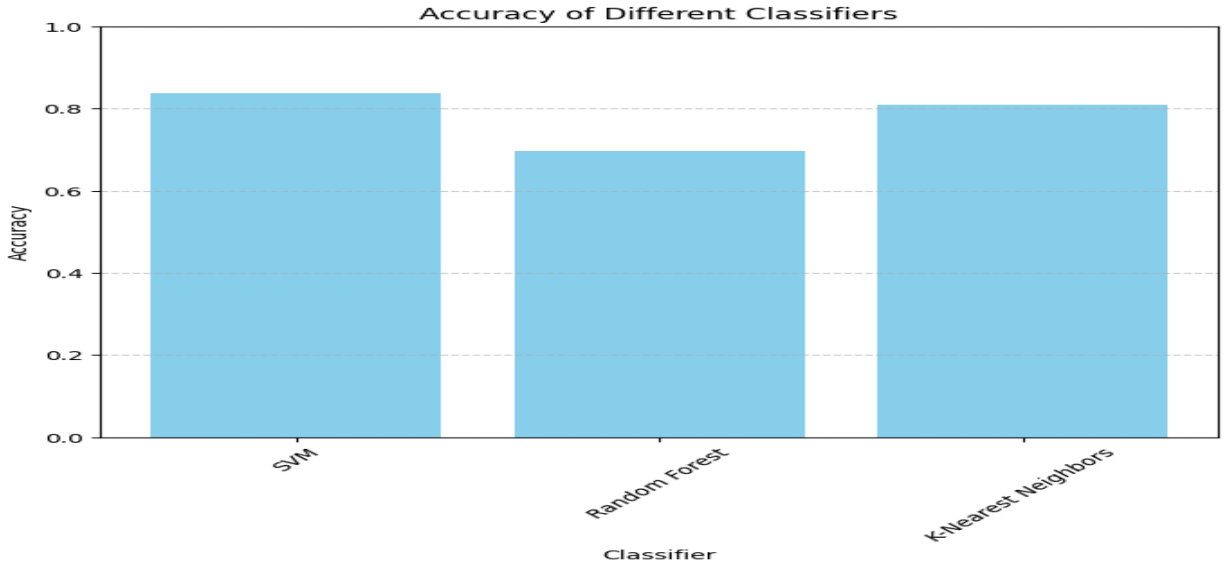

Figure 5. Accuracies comparison

5. Conclusions

Our study delved into the performance evaluation of K-Nearest Neighbors (KNN), Support Vector Machine (SVM), and Random Forest (RF) algorithms in classifying Alzheimer's disease. The results revealed that KNN achieved the highest accuracy among the three, while SVM and RF demonstrated competitive performance with varying computational efficiencies. However, SVM, despite its accuracy, required longer computation times compared to KNN and RF. RF's utilization of ensemble learning contributed to its robustness, albeit with a marginally lower accuracy rate.

These outcomes emphasize the significance of considering trade-offs between accuracy, computational efficiency, and model robustness when choosing classification algorithms. Future research endeavors aim to explore hybrid methodologies that harness the strengths of multiple algorithms to enhance the detection and classification of Alzheimer's disease. Additionally, integrating deep learning models for feature extraction with traditional machine learning classifiers holds potential to enhance classification accuracy and efficiency. Furthermore, expanding the dataset size and incorporating more diverse features could improve model generalization and performance across various patient cohorts. Overall, these research directions offer promising avenues for advancing the diagnosis and management of Alzheimer's disease.

References

1. W. E. Klunk et al., "Imaging brain amyloid in Alzheimer's disease with Pittsburgh Compound-B," Ann. Neurol. Off. J. Am. Neurol. Assoc. Child Neurol. Soc., vol. 55, no. 3, pp. 306–319, 2004.
2. M. Marquié et al., "Validating novel tau positron emission tomography tracer [F-18]-AV-1451 (T807) on postmortem brain tissue," Ann. Neurol., vol. 78, no. 5, pp. 787–800, 2015.
3. N. Schuff et al., "MRI of hippocampal volume loss in early Alzheimer's disease in relation to ApoE genotype and biomarkers," Brain, vol. 132, no. 4, pp. 1067–1077, 2009.
4. R. Kadri, B. Bouaziz, M. Tmar, and F. Gargouri, "Multimodal deep learning based on the combination of EfficientNetV2 and ViT for Alzheimer's disease early diagnosis enhanced by SAGAN data augmentation," Int J Comput Inf Syst Ind Manag Appl, vol. 14, pp. 313–325, 2022.
5. S. S. Shastri, A. Bhadrashetty, and S. Kulkarni, "Detection and Classification of Alzheimer's Disease by Employing CNN," Int J Intell Syst Appl, vol. 15, pp. 14–22, 2023.
6. C. Zhang, W. Fan, B. Wang, C. Chen, and H. Li, "Self-paced semi-supervised feature selection with application to multi-modal Alzheimer's disease classification," Inf. Fusion, p. 102345, 2024.
7. X. Hao et al., "Multi-modal neuroimaging feature selection with consistent metric constraint for diagnosis of Alzheimer's disease," Med. Image Anal., vol. 60, p. 101625, 2020.
8. C. R. Jack Jr et al., "NIA-AA research framework: toward a biological definition of Alzheimer's disease," Alzheimers Dement., vol. 14, no. 4, pp. 535–562, 2018.
9. T. Tong et al., "Multiple instance learning for classification of dementia in brain MRI," Med. Image Anal., vol. 18, no. 5, pp. 808–818, 2014.
10. P. Balaji, M. A. Chaurasia, S. M. Bilfaqih, A. Muniasamy, and L. E. G. Alsid, "Hybridized deep learning approach for detecting Alzheimer's disease," Biomedicines, vol. 11, no. 1, p. 149, 2023.
11. J. Islam and Y. Zhang, "Brain MRI analysis for Alzheimer's disease diagnosis using an ensemble system of deep convolutional neural networks," Brain Inform., vol. 5, pp. 1–14, 2018.
12. S. L. Warren and A. A. Moustafa, "Functional magnetic resonance imaging, deep learning, and Alzheimer's disease: A systematic review," J. Neuroimaging, vol. 33, no. 1, pp. 5–18, 2023.
13. D. Prakash et al., "A comparative study of Alzheimer's disease classification using multiple transfer learning models," J. Multimed. Inf. Syst., vol. 6, no. 4, pp. 209–216, 2019.
14. D. Holilah, A. Bustamam, and D. Sarwinda, "Detection of Alzheimer's disease with segmentation approach using K-Means Clustering and Watershed Method of MRI image," in Journal of Physics: Conference Series, IOP Publishing, 2021, p. 012009.
15. E. U. Haq, Q. Yong, Z. Yuan, H. Jianjun, and R. U. Haq, "Multimodal Fusion Diagnosis of the Alzheimer's Disease Via Lightweight CNN-LSTM Model Using Magnetic Resonance Imaging (MRI)," Available SSRN 4719918.
16. C.-N. Jiao, Y.-L. Gao, D.-H. Ge, J. Shang, and J.-X. Liu, "Multi-modal imaging genetics data fusion by deep auto-encoder and self-representation network for Alzheimer's disease diagnosis and biomarkers extraction," Eng. Appl. Artif. Intell., vol. 130, p. 107782, 2024.
17. G. Castellano, A. Esposito, E. Lella, G. Montanaro, and G. Vessio, "Automated detection of Alzheimer's disease: a multi-modal approach with 3D MRI and amyloid PET," Sci. Rep., vol. 14, no. 1, p. 5210, 2024.
18. M. Trinh, R. Shahbaba, C. Stark, and Y. Ren, "Alzheimer's disease detection using data fusion with a deep supervised encoder," Front. Dement., vol. 3, p. 1332928, 2024.
19. Y. Tu, S. Lin, J. Qiao, Y. Zhuang, Z. Wang, and D. Wang, "Multimodal fusion diagnosis of Alzheimer's disease based on FDG-PET generation," Biomed. Signal Process. Control, vol. 89, p. 105709, 2024.
20. M. Zaabi, N. Smaoui, H. Derbel, and W. Hariri, "Alzheimer's disease detection using convolutional neural networks and transfer learning based methods," in 2020 17th International Multi-Conference on Systems, Signals & Devices (SSD), IEEE, 2020, pp. 939–943.
21. Latif, J., Xiao, C., Imran, A., & Tu, S. (2019, January). Medical imaging using machine learning and deep learning algorithms: a review. In 2019 2nd International Conference on Computing, mathematics and engineering technologies (iCoMET) (pp. 1-5). IEEE.
22. Imran, A., Li, J., Pei, Y., Yang, J. J., & Wang, Q. (2019). Comparative analysis of vessel segmentation techniques in retinal images. IEEE Access, 7, 114862-114887.
23. Mokbal, F. M. M., Dan, W., Imran, A., Jiuchuan, L., Akhtar, F., & Xiaoxi, W. (2019). MLPXSS: an integrated XSS-based attack detection scheme in web applications using multilayer perceptron technique. IEEE Access, 7, 100567-100580.
24. Mahmood, T., Li, J., Pei, Y., Akhtar, F., Imran, A., & Rehman, K. U. (2020). A brief survey on breast cancer diagnostic with deep learning schemes using multi-image modalities. IEEE Access, 8, 165779-165809.
25. Li, J., Xu, X., Guan, Y., Imran, A., Liu, B., Zhang, L., ... & Xie, L. (2018, October). Automatic cataract diagnosis by image-based interpretability. In 2018 IEEE international conference on systems, man, and cybernetics (SMC) (pp. 3964-3969). IEEE.
26. Khan, U., An, Z. Y., & Imran, A. (2020). A blockchain ethereum technology-enabled digital content: development of trading and sharing economy data. IEEE access, 8, 217045-217056.
27. Latif, J., Xiao, C., Tu, S., Rehman, S. U., Imran, A., & Bilal, A. (2020). Implementation and use of disease diagnosis systems for electronic medical records based on machine learning: A complete review. IEEE Access, 8, 150489-150513.

28. Imran, A., Li, J., Pei, Y., Akhtar, F., Mahmood, T., & Zhang, L. (2021). Fundus image-based cataract classification using a hybrid convolutional and recurrent neural network. The Visual Computer, 37, 2407-2417.
29. Imran, A., Li, J., Pei, Y., Akhtar, F., Yang, J. J., & Dang, Y. (2020). Automated identification of cataract severity using retinal fundus images. Computer Methods in Biomechanics and Biomedical Engineering: Imaging & Visualization, 8(6), 691-698.
30. Imran, A., Li, J., Pei, Y., Akhtar, F., Yang, J. J., & Wang, Q. (2019, December). Cataract detection and grading with retinal images using SOM-RBF neural network. In 2019 IEEE Symposium Series on Computational Intelligence (SSCI) (pp. 2626-2632). IEEE.
31. Imran, A., Aslam, W., & Ullah, M. I. (2017). Quantitative prediction of offensiveness using text mining of twitter data. Sindh University Research Journal-SURJ (Science Series), 49(1).
32. Rahman, H., Bukht, T. F. N., Imran, A., Tariq, J., Tu, S., & Alzahrani, A. (2022). A Deep Learning Approach for Liver and Tumor Segmentation in CT Images Using ResUNet. Bioengineering, 9(8), 368.
33. Mahmood, T., Li, J., Pei, Y., Akhtar, F., Imran, A., & Yaqub, M. (2021). An automatic detection and localization of mammographic microcalcifications ROI with multi-scale features using the radiomics analysis approach. Cancers, 13(23), 5916.
34. Bilal, A., Sun, G., Mazhar, S., & Imran, A. (2022). Improved Grey Wolf Optimization-Based Feature Selection and Classification Using CNN for Diabetic Retinopathy Detection. In Evolutionary Computing and Mobile Sustainable Networks: Proceedings of ICECMSN 2021 (pp. 1-14). Singapore: Springer Singapore.
35. Imran, A., Nasir, A., Bilal, M., Sun, G., Alzahrani, A., & Almuhaimeed, A. (2022). Skin Cancer Detection Using Combined Decision of Deep Learners. IEEE Access, 10, 118198-118212.
36. Arooj, S., Rehman, S. U., Imran, A., Almuhaimeed, A., Alzahrani, A. K., & Alzahrani, A. (2022). A Deep Convolutional Neural Network for the Early Detection of Heart Disease. Biomedicines, 10(11), 2796.
37. Abbas, A., Imran, A., Al-Aloosy, A. A. N., Fahim, S., Alzahrani, A., & Muzaffar, S. K. (2022, October). Heart Failure Prediction Using Machine learning Approaches. In 2022 Mohammad Ali Jinnah University International Conference on Computing (MAJICC) (pp. 1-7). IEEE.
38. Li, J., Hu, Q., Imran, A., Zhang, L., Yang, J. J., & Wang, Q. (2018, July). Vessel recognition of retinal fundus images based on fully convolutional network. In 2018 IEEE 42nd annual computer software and applications conference (COMPSAC) (Vol. 2, pp. 413-418). IEEE.